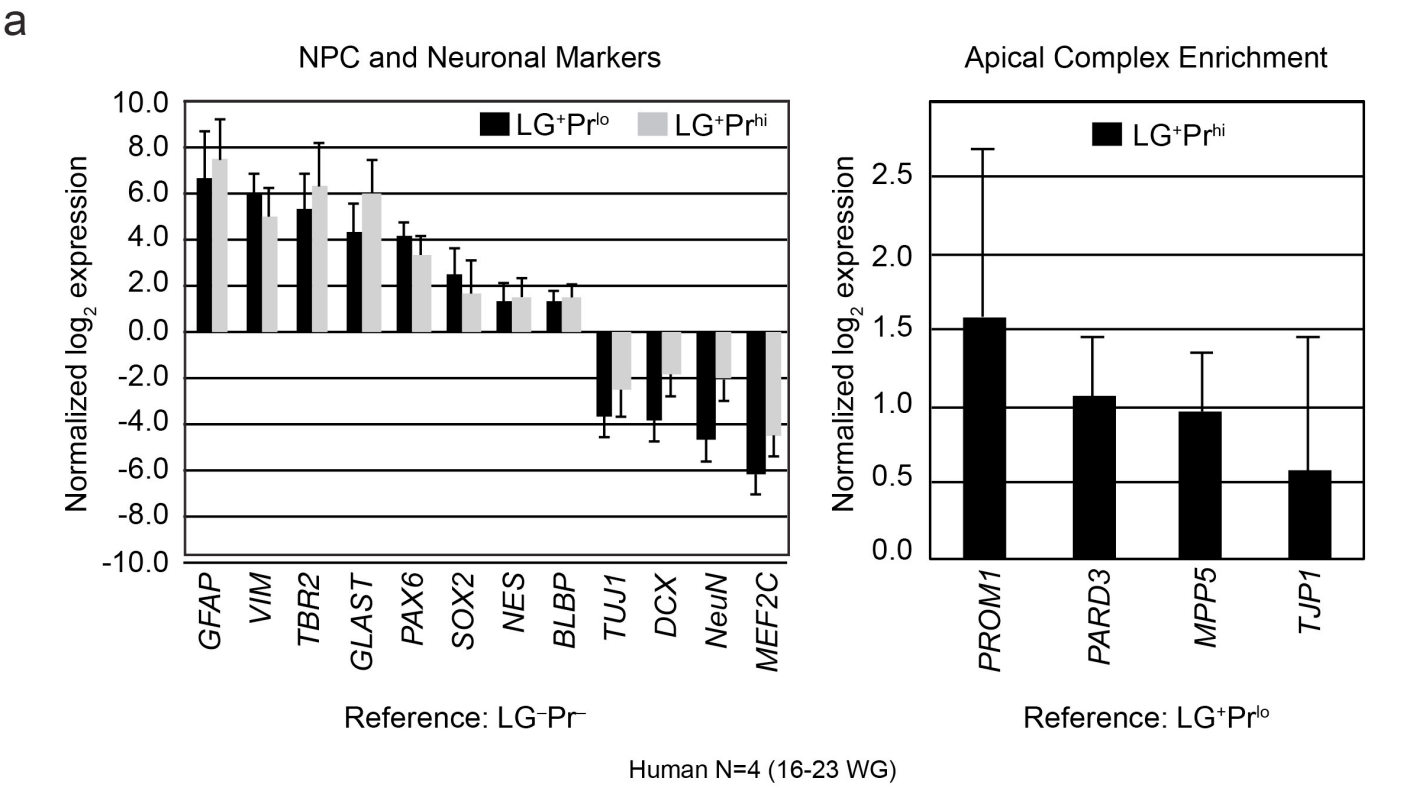

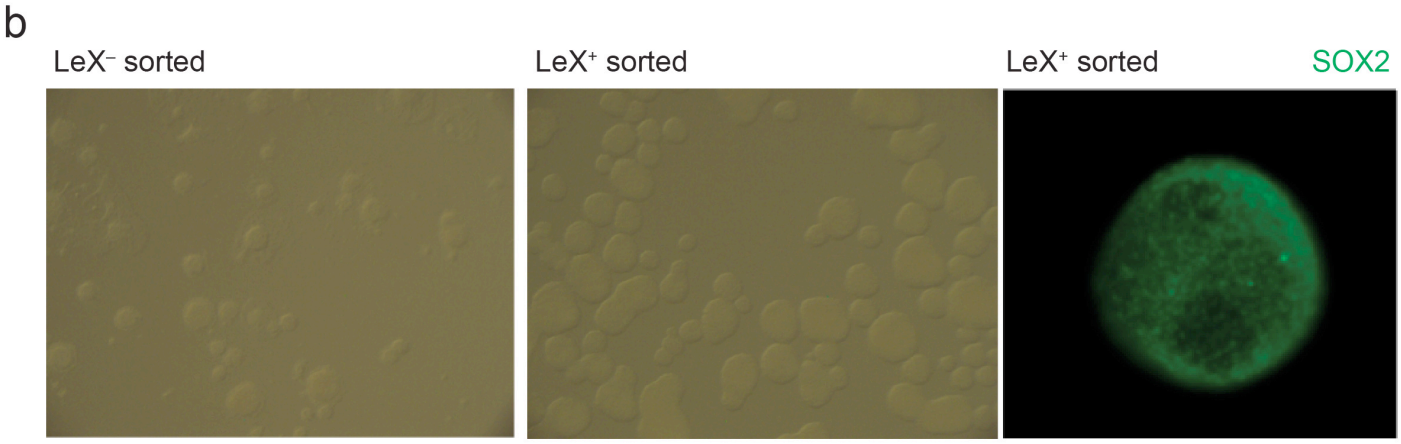

Supplementary Figure 1

Isolation of human RGC subpopulations by FACS

a, Both LG^+Pr^{hi} and LG^+Pr^{lo} subpopulations are enriched for known RGC-expressed genes (*GFAP, VIM, GLAST, PAX6, SOX2, BLBP*), and depleted for neuronal markers (*DCX, TUJ1, NeuN, MEF2C*). The LG^+Pr^{hi} subpopulation was enriched relative to the LG^+Pr^{lo} subpopulation for *PROM1* transcript as well as three other transcripts encoding apical membrane domain-specific proteins (*PARD3 [Par3], TJP1 [ZO-1], MPP5 [Pals]*). Data represents four biological replicates (mean ± SEM) ranging from 16 WG to 23 WG. **b,** Primary neurospheres derived from LeX^- and LeX^+ cells sorted from dissociated human fetal cortex. Neurospheres were serially passaged at clonal density and immunolabeled for RGC marker SOX2.

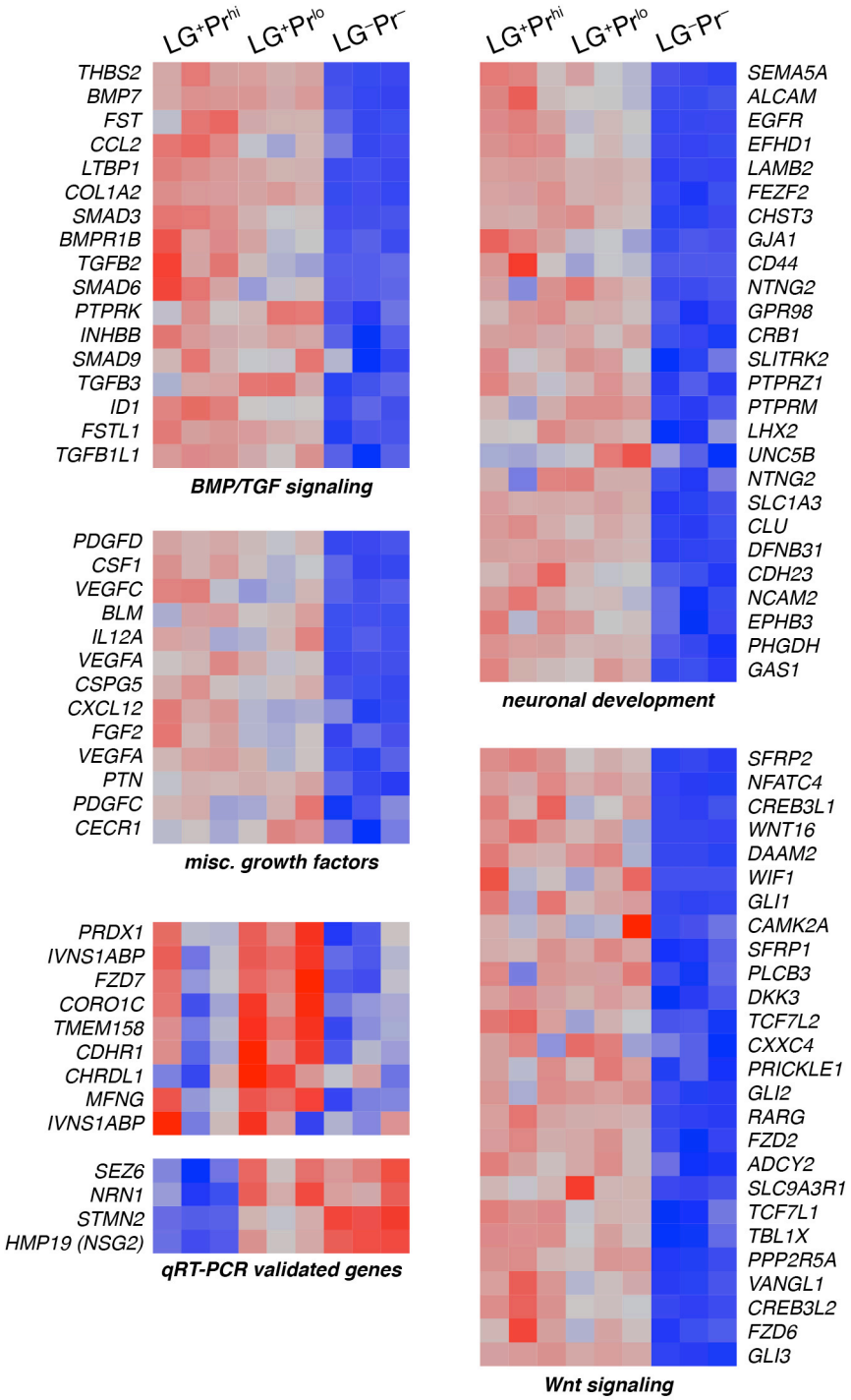

Supplementary Figure 2

Gene set enrichment in human RGC subpopulations

Gene set enrichment analysis confirmed the RGC progenitor nature of both the $LG^{+}Pr^{hi}$ and $LG^{+}Pr^{lo}$ subpopulations, with enrichment of important progenitor signaling pathways (e.g. Wnt/Bmp/Tgf) and gene ontology terms (cell cycle control, neural development) in both subpopulations relative to $LG^{-}Pr^{-}$ neurons and other cell types.

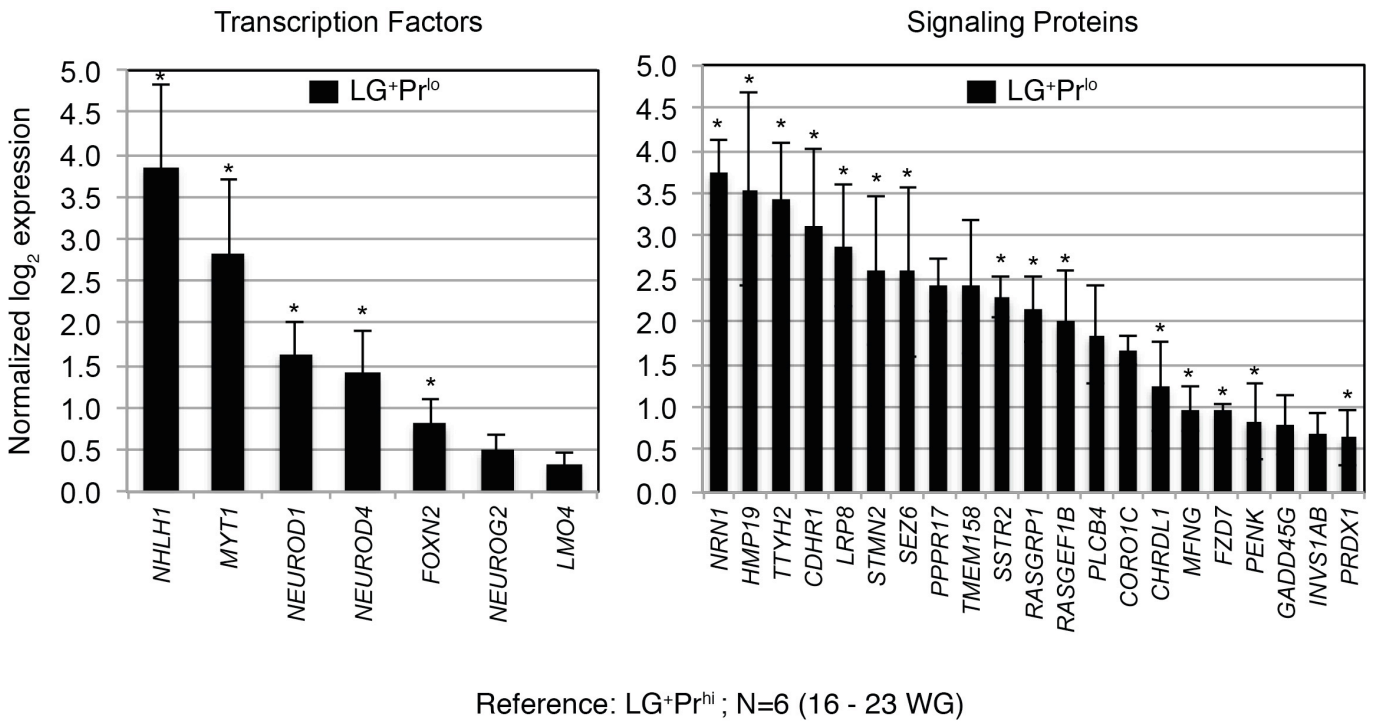

Supplementary Figure 3

Selected $LG^{+}Pr^{lo}$-enriched candidate non-apical RGC genes validated by qRT-PCR in independent biological replicates of FACS-purified human fetal RGC.

Relative expression levels in the $LG^{+}Pr^{lo}$ subpopulation compared to $LG^{+}Pr^{hi}$ after normalization to housekeeping genes *ACTB* and *GAPDH*. Data represents six biological replicates (mean ± SEM) ranging from 16 WG to 23 WG (asterisk denotes $p < 0.05$, paired t-test; n=6, max p=0.045, all others were lower).

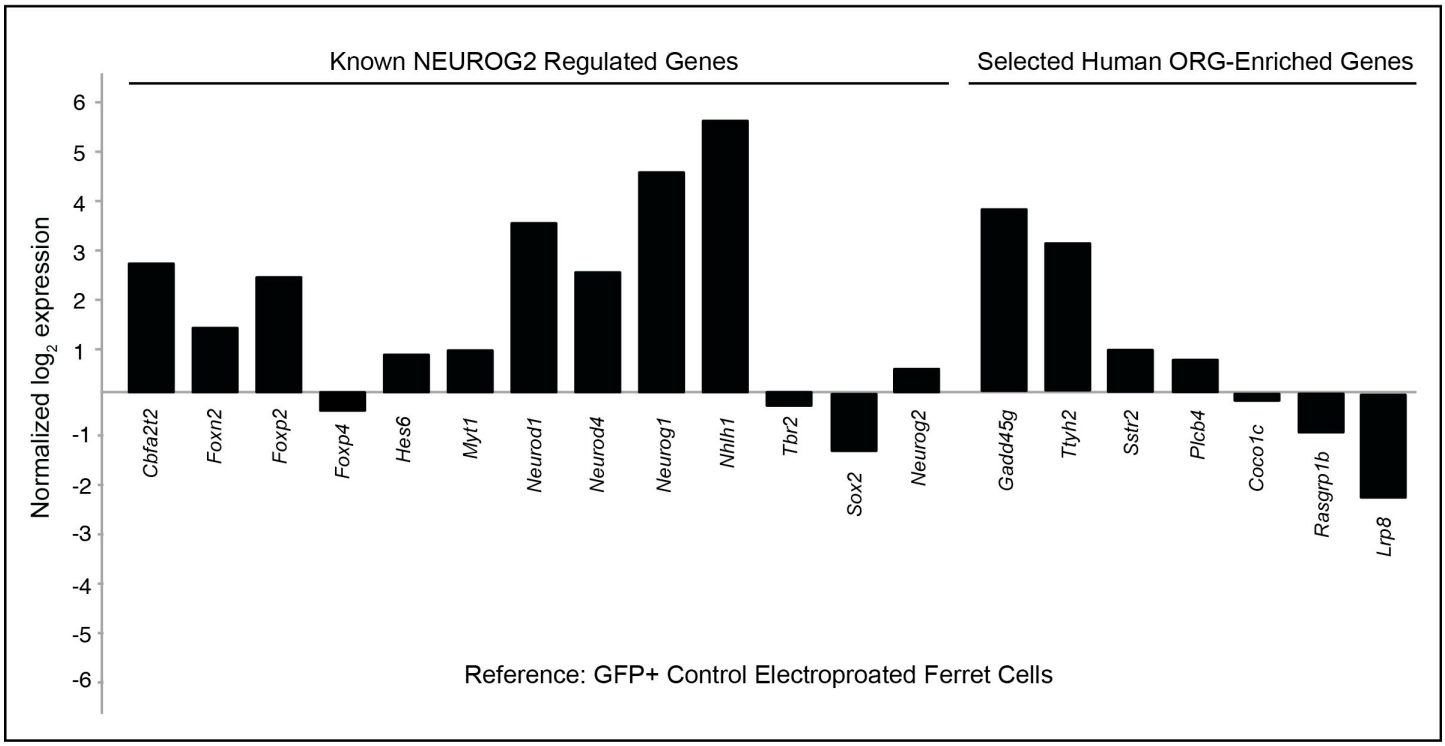

Supplementary Figure 4

Upregulation of proneural neurogenin targets in NEUROG2-VP16 electroporated ferret cells

In vivo delivery of GFP control and *NEUROG2-VP16* constructs to ferret apical RGCs was performed by intraventricular injection and electroporation in neonatal ferret kits (n=2 per condition at postnatal day 1) as described in Figure 2. After 48 hours post-electroporation, electroporated cells were isolated for qRT-PCR analysis by enzymatic dissociation and FACS using their GFP fluorescence. Relative to GFP+ control electroporated cells, *NEUROG2-VP16* expressing cells showed upregulation of many previously described NEUROG2 effector genes including *Cbfa2t2*, *Foxn2*, *Foxp2*, *Hes6*, *Myt1*, *Neurod1*, *Neurod4*, *Neurog1*, and *Nhlh1,* and down-regulation of *Sox2*. In addition, we also tested expression of ferret orthologs of human ORG-enriched genes and found that several including *Gadd45g*, *Ttyh2*, *Sstr2*, and *Plcb4* were also upregulated in NEUROG2-VP16 cells compared to controls.

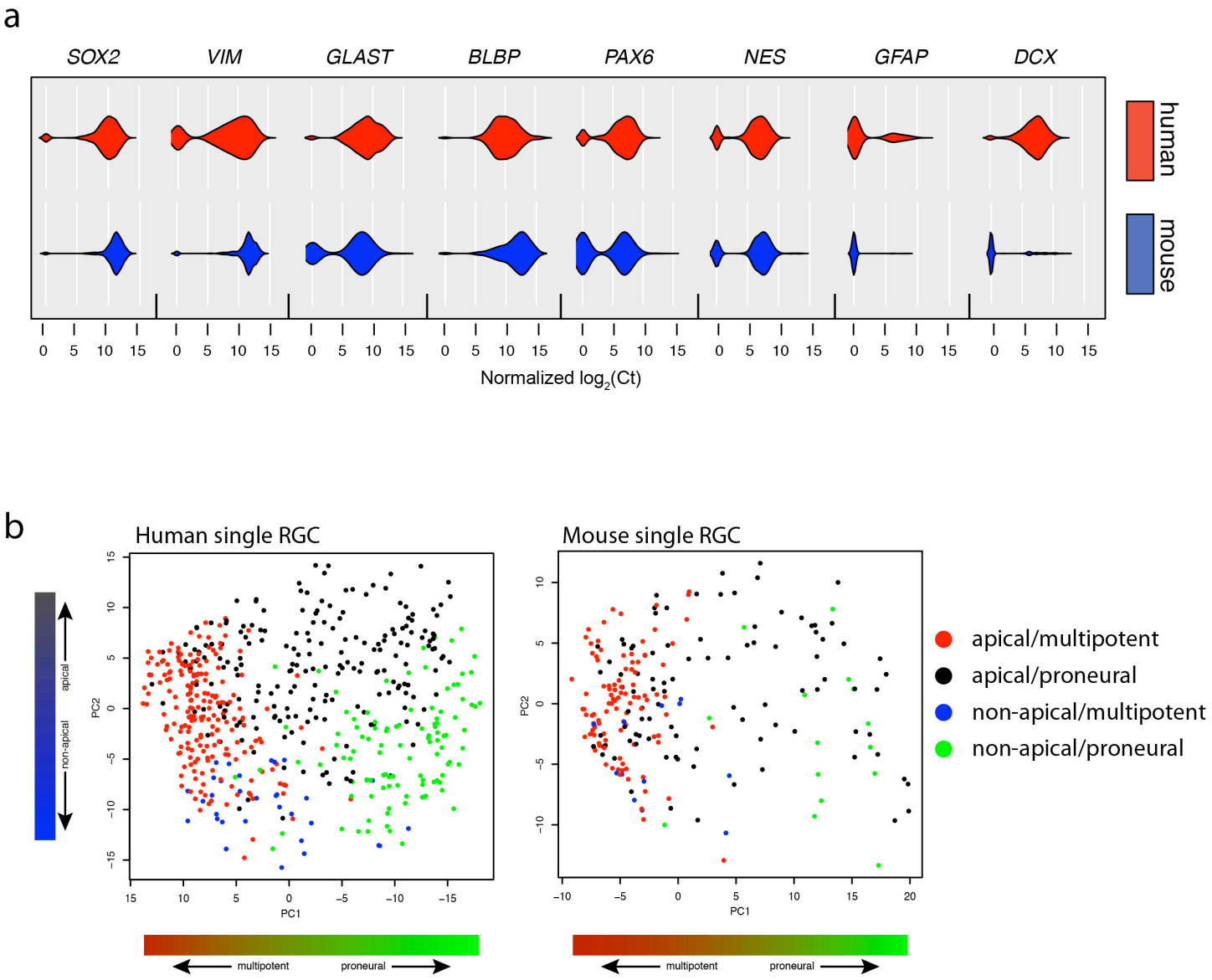

Supplementary Figure 5

Single-cell expression profiles of human and mouse RGC

a, Violin plots of RGC marker gene expression in human and mouse single sorted RGC reveals largely similar pattern of gene expression for RGC markers including *SOX2, VIM, GLAST, BLBP, PAX6, NES*. Interestingly, significant numbers of human RGC express *GFAP* and *DCX* but these genes are nearly absent in mouse RGC. **b,** Principle component analysis of 546 human (left) and 226 mouse (right) single RGC indicates distinct distributions of transcriptional states in human compared to mouse RGC. Here, "apical" is defined by expression of at least two of the four apical complex marker transcripts, and "proneural" by expression of at least two of the four Neurogenin pathway genes. In both species, the first PC (x-axis) reflects the proneural+/– dimension, with "multipotent" (presumptively pre-Neurogenin-pathway-expressing) RGC tending towards the left (red and blue cells) and proneural RGC on the right (black and green cells). Human cortex contains a greater proportion of proneural RGC, whereas mouse has fewer proneural cells which are less distinct, as indicated by the greater overlap of black and red cells in the mouse. In addition, human cortex displays far more non-apical (blue and green) cells than mouse, which again are more distinct from the apical (red and black) cells along the second PC (y-axis). In contrast, mouse non-apical RGC (blue and green) are scarce and not transcriptionally distinct from apical cells, as indicated by the lack of separation along the y-axis.

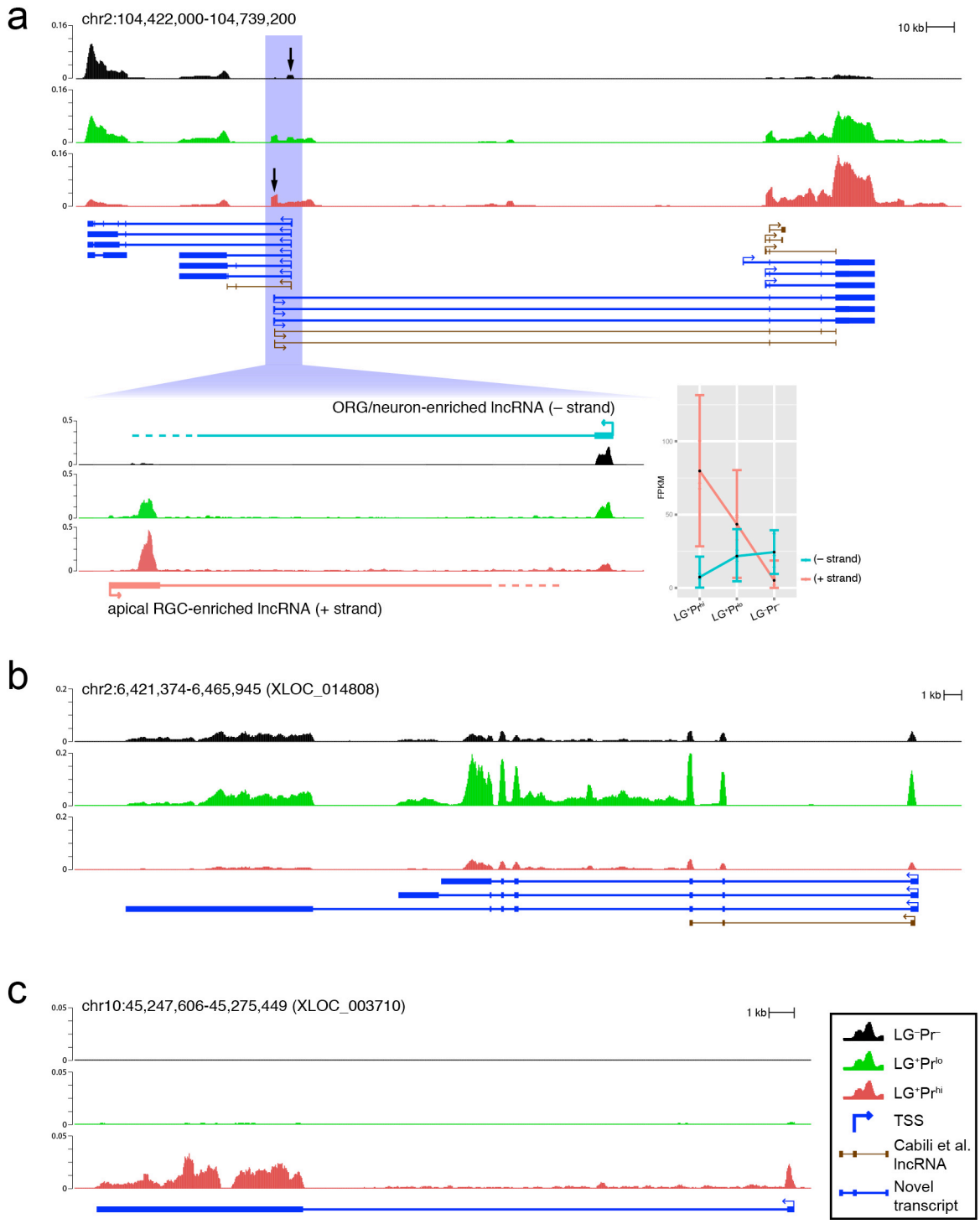

Supplementary Figure 6

Differential expression of novel unannotated lncRNAs in human RGC subtypes

RNA-seq reads displayed in genomic context for the $LG^{+}Pr^{hi}$ apical RGC (red), $LG^{+}Pr^{lo}$ ORG (green), and $LG^{-}Pr^{-}$ cells (black). Novel transcripts assembled from the RNA-seq data are shown in blue, and previously catalogued lncRNA transcripts are shown in brown[39]. **a,** Two intergenic lncRNAs on chromosome 2 with distinct expression patterns in the human fetal cortex share a bidirectional promoter and overlap at their 5' ends. The plus-strand lncRNA is enriched in apical RGC, whereas the minus-strand lncRNA is relatively enriched

in ORG and neurons. Blue boxed region highlights the overlapping transcription start sites (TSS), and is enlarged below. Black arrows indicate read peaks from each strand's TSS. Bottom part of **(a)** shows the promoter at higher magnification, with expression levels of the two lncRNAs (in FPKM) plotted at right. **b,** Example of an ORG-enriched lncRNA. Multiple alternatively spliced isoforms of this multi-exon locus are expressed in all cell types assayed, but are significantly enriched in the $LG^{+}Pr^{lo}$ non-apical subpopulation. A partial transcript overlapping the 5' end of the locus was previously detected by ultra-high depth RNA sequencing[39]; our data demonstrate that even low-abundance transcripts can be captured and fully reconstructed from an order of magnitude fewer reads when RNA is sequenced from the specific cell types that express the gene, rather than from heterogeneous bulk tissue. **c,** Example of a novel apical RGC-specific intergenic transcript not detected by previous deep-sequencing experiments.

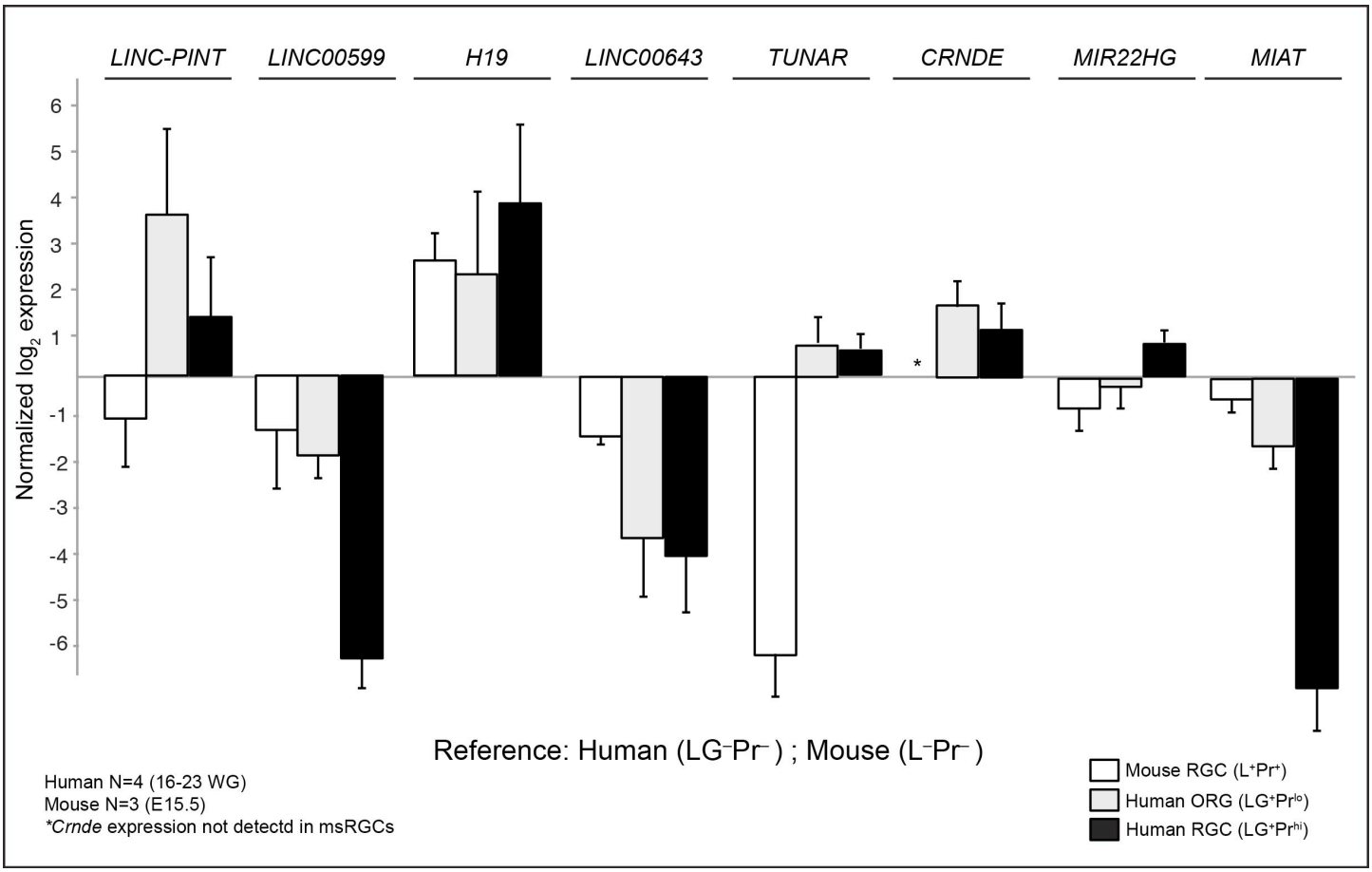

Supplementary Figure 7

Differential enrichment of lncRNAs in human and mouse RGC populations

We performed qRT-PCR of several conserved lncRNAs in FACS-purified human (n=4 biological replicates ranging from 16 WG to 23 WG) and mouse RGC populations (n=3 from E15.5) comparing human ORG ($LG^{+}Pr^{lo}$) and apical RGC ($LG^{+}Pr^{hi}$) with neurons ($LG^{-}Pr^{-}$) and mouse RGC ($L^{+}Pr^{+}$) with neurons ($L^{-}Pr^{-}$) (mean ± SEM). We find that several conserved lncRNAs including *LINC-PINT*, *TUNAR*, *CRNDE*, *MIR22HG* are enriched in human RGC progenitor populations but depleted in mouse RGC suggesting potentially divergent roles in human radial progenitor evolution and function.

Supplementary Table 1 | List of human fetal specimens collected, gestational ages, and studies performed.

Sample	Age (WG)	Studies Performed
FB018	23	Candidate validation (qRT-PCR)
FB044	16	Candidate validation (qRT-PCR)
FB025	23	Candidate validation (qRT-PCR)
FB035	18	RNA-seq
FB036	18	Neurosphere culturing
FB031	19	Candidate validation (qRT-PCR)
FB032	18	RNA-seq
FB033	19	RNA-seq
FB040	20	Candidate validation (qRT-PCR), Single-cell expression profiling (Biomark)
FB043	17	Candidate validation (qRT-PCR), Single-cell expression profiling (Biomark)
FB024	20	Single-cell expression profiling (Biomark)
FB049	16	Single-cell expression profiling (Biomark)
FB053	21	Single-cell expression profiling (Biomark)
FB066	18	Single-cell expression profiling (Biomark)
FB068	20	Single-cell expression profiling (Biomark)

Supplementary Table 2 | Comparison of the present RNA-seq data to previous transcriptome studies of fetal cortical progenitors.

Genes expressed in human but not mouse RGC (Lui, Nowakowski et al., 2014)

Gene Symbol	Human Progenitor Expression Pattern (FACS-RNA-seq)	Ferret RGC Expression Level (fpkm)
ABHD3	pan-RGC enriched	0.8
ASAP3	pan-RGC enriched	14.4
BMP7	pan-RGC enriched	25.7
C5	pan-RGC enriched	0.2
C8orf4	pan-RGC enriched	22.9
FAM107A	pan-RGC enriched	1.9
FOXN4	pan-RGC enriched	9.7
ITGA2	apical RGC > ORG	30.2
LRIG3	pan-RGC enriched	7.1
LRRC17	pan-RGC enriched	0.4
PAM	pan-RGC enriched	22.9
PDGFD	pan-RGC enriched	0.1
PDGFRB	apical RGC > ORG	14.9
PDLIM3	pan-RGC enriched	17.7
RFTN2	pan-RGC enriched	43.0
SLC2A10	pan-RGC enriched	3.1
SP110	pan-RGC enriched	0.3
STOX1	pan-RGC enriched	20.8
ZC3HAV1	pan-RGC enriched	2.8

n.a., not annotated

Human OSVZ-enriched genes (Miller, Ding et al., 2014)

Gene Symbol	Human Progenitor Expression Pattern (FACS-RNA-seq)	Ferret RGC Expression Level (fpkm)
LRP3	neuron-enriched	34.7
HNRNPA3	no significant difference	n.a.
HNRNPH3	no significant difference	151.3
MT1F	no significant difference	n.a.
MT1G	no significant difference	n.a.
MT1H	no significant difference	n.a.
POLR2J2	no significant difference	n.a.
PSMC3IP	no significant difference	30.7

n.a., not annotated

Human OSVZ-enriched genes (Fietz et al., 2012)

Gene Symbol	Human Progenitor Expression Pattern (FACS-RNA-seq)	Ferret RGC Expression Level (fpkm)
Ankrd23	no significant difference	n.a.
C1orf111	neuron-enriched	0.5

Cerkl	pan-RGC enriched	0.6
Cldn11	apical RGC > ORG	1.1
Dcbld1	no significant difference	0.0
Dclk3	strong_late_ON	0.1
Fkbp11	no significant difference	8.4
Gigyf2	no significant difference	18.7
Itih4	no significant difference	0.0
KIAA1324	neuron-enriched	16.1
KIAA1324L	neuron-enriched	n.a.
Lims2	apical RGC > ORG	0.7
Nipsnap1	no significant difference	42.6
Olig1	apical RGC > ORG > neurons	n.a.
Parp10	no significant difference	n.a.
Pcbp2	no significant difference	541.3
Prss12	strong_late_ON	11.7
Sox10	apical RGC > ORG	1.0
Tmem88	neuron-enriched	n.a.
TPGS2	no significant difference	20.1

n.a., not annotated

Embryonic mouse cortex single-cell profiling "cluster II/III genes" (Kawaguchi et al., 2008)

Gene Symbol	Human Progenitor Expression Pattern (FACS-RNA-seq)	Ferret RGC Expression Level (fpkm)
Afap1	no significant difference	19.3
CLVS1	no significant difference	1.3
Coro1c	ORG-enriched	46.9
Cxcl12	apical RGC-enriched	0.3
Elav2	no significant difference	n.a.
Elav4	no significant difference	n.a.
Eomes (Tbr2)	pan-RGC enriched	173.5
Gadd45G	ORG & neurons > apical RGC	52.8
Hes6	pan-RGC enriched	n.a.
Insm1	ORG-enriched	12.6
Lrp8	ORG & neurons > apical RGC	42.8
Lrrn3	no significant difference	60.8
Mfng	pan-RGC enriched	41.5
Mgat5b	neuron-enriched	0.8
Myt1	ORG & neurons > apical RGC	14.0
Neurod1	ORG & neurons > apical RGC	22.1
Neurog2	no significant difference	155.0
Nrn1	ORG & neurons > apical RGC	19.4
Rasgef1b	ORG & neurons > apical RGC	8.2
Rwdd3	no significant difference	5.2
Sdc3	no significant difference	61.4
Serping1	no significant difference	2.9
Sertad4	pan-RGC enriched	6.4
Slc17a6	ORG & neurons > apical RGC	2.0
Sorbs2	ORG & neurons > apical RGC	59.9
Sstr2	ORG-enriched	n.a.
Trp53inp1	no significant difference	n.a.

n.a., not annotated

Supplementary Table 2 | Comparison of the present RNA-seq data to previous transcriptome studies of fetal cortical progenitors.

Several recent studies have examined the transcriptional signature of human fetal germinal zones using manually or laser capture-assisted microdissection techniques[13-15]. Here we list the central findings of several of these papers and the differential expression patterns we observe for these genes using our FACS-RNA-seq strategy (middle column). We also report the expression levels (fpkm) of these genes in ferret RGC (right column), noting that many genes are conserved in their progenitor expression but some, such as *PDGFD*, are not. Most notable in this analysis is the absence of ORG-enriched genes from previous transcriptome assays of the human OSVZ[13,14], where most ORG are located. We attribute this discrepancy to the highly heterogeneous cellular composition of the OSVZ, which in addition to ORG harbors multipolar intermediate progenitors, radially migrating postmitotic neurons generated in both the VZ and SVZ, and tangentially migrating interneurons originated from the ganglionic eminences. Furthermore, our single-cell data demonstrate additional transcriptional heterogeneity even within ORG, which further confounds efforts to profile these cells from bulk tissue samples. Thus none of the ORG-enriched genes identified in our current study have previously been associated with this cell type by other methods. Remarkably, however, at least 8 genes that we found as having significant or trending human ORG enrichment were previously described in a single-cell expression microarray analysis of the embryonic mouse cortex[46] (genes marked in red bold text in the bottom section). These authors also showed by *in situ* hybridization in E14 mouse cortex that several human ORG-enriched genes are expressed in a narrow band of cells at the VZ-SVZ border in mouse, in contrast to the OSVZ location of most ORG in human and other ORG-abundant species. We interpret these results as indicating that some human ORG-enriched genes

are also expressed in mouse progenitors during the transition from VZ RGC to SVZ IP, as has been clearly demonstrated for *Neurog2*[23], thus further supporting our conclusion that the ORG transcriptional signature reflects a transitional developmental state.

Supplementary Table 3: Species used for multi-species alignment

Common name	Latin binomial
Primate subset	
Baboon	*Papio hamadryas*
Bushbaby	*Otolemur garnettii*
Chimp	*Pan troglodytes*
Crab-eating macaque	*Macaca fascicularis*
Gibbon	*Nomascus leucogenys*
Gorilla	*Gorilla gorilla gorilla*
Green monkey	*Chlorocebus sabaeus*
Human	*Homo sapiens*
Marmoset	*Callithrix jacchus*
Orangutan	*Pongo pygmaeus abelii*
Rhesus	*Macaca mulatta*
Squirrel monkey	*Saimiri boliviensis*
Euarchontoglires subset	
Brush-tailed rat	*Octodon degus*
Chinchilla	*Chinchilla lanigera*
Chinese hamster	*Cricetulus griseus*
Chinese tree shrew	*Tupaia chinensis*
Golden hamster	*Mesocricetus auratus*
Guinea pig	*Cavia porcellus*
Lesser Egyptian jerboa	*Jaculus jaculus*
Mouse	*Mus musculus*
Naked mole-rat	*Heterocephalus glaber*
Pika	*Ochotona princeps*
Prairie vole	*Microtus ochrogaster*
Rabbit	*Oryctolagus cuniculus*
Rat	*Rattus norvegicus*
Squirrel	*Spermophilus tridecemlineatus*
Laurasiatheria subset	
Alpaca	*Vicugna pacos*
Bactrian camel	*Camelus ferus*
Big brown bat	*Eptesicus fuscus*
Black flying-fox	*Pteropus alecto*
Cat	*Felis catus*
Cow	*Bos taurus*
David's myotis bat	*Myotis davidii*
Dog	*Canis lupus familiaris*
Dolphin	*Tursiops truncatus*
Domestic goat	*Capra hircus*
Ferret	*Mustela putorius furo*
Hedgehog	*Erinaceus europaeus*
Horse	*Equus caballus*
Killer whale	*Orcinus orca*
Megabat	*Pteropus vampyrus*
Microbat	*Myotis lucifugus*
Pacific walrus	*Odobenus rosmarus divergens*
Panda	*Ailuropoda melanoleuca*
Pig	*Sus scrofa*
Sheep	*Ovis aries*
Shrew	*Sorex araneus*
Star-nosed mole	*Condylura cristata*
Tibetan antelope	*Pantholops hodgsonii*
Weddell seal	*Leptonychotes weddellii*
White rhinoceros	*Ceratotherium simum*
Afrotheria subset	
Aardvark	*Orycteropus afer afer*
Cape elephant shrew	*Elephantulus edwardii*
Cape golden mole	*Chrysochloris asiatica*
Elephant	*Loxodonta africana*
Manatee	*Trichechus manatus latirostris*
Tenrec	*Echinops telfairi*
Mammal subset	
Armadillo	*Dasypus novemcinctus*